Simulation of the QinetiQ T6 Engine Ion Optics and Comparison to the Experimental Data

IEPC-2015-220／ISTS-2015-b-220

Presented at Joint Conference of 30th International Symposium on Space Technology and Science 34th International Electric Propulsion Conference and 6th Nano-satellite Symposium, Hyogo-Kobe, Japan July 4 – 10, 2015

Michele Coletti[1],
Mars Space Ltd, Southampton, SO145FE, UK

The QinetiQ T6 ion engine is currently being qualified for the European Space Agency BepiColombo mission to operate at thrust levels between 75 and 145 mN. Moreover as part of a small ESA activity the T6 ion engine performance has been tested at low thrust levels (from 30 to 50 mN) compatible with the Marco Polo R (MPR) mission. In this paper the T6 ion engine has been numerically simulated using the FFX codes. Firstly the code has been validated with respect to the existing Bepi experimental data. After this the 0D model used to derive the density and temperature profiles at low thrust levels (where no measurement are currently available) has been presented and tuned using existing Bepi measurements. Finally the T6 ion engine lifetime has been simulated at thrust levels ranging from 30 to 145mN. According to these simulations the T6 has been found to deliver lifetimes well in excess of 50khrs at all thrust levels. The lifetime simulations results have been critically reviewed.

Nomenclature

A^i	=	effective area of the discharge chamber surfaces at cathodic potential collecting ions
A_p	=	the effective area of the anode collecting primary electrons
I_{BEAM}	=	beam current
I_{ACC}	=	accel grid current
n_e	=	plasma density
n++	=	percentage of double ions
J_{beam}	=	beamlet current density
J_{acc}	=	accel gridlet current density
r_g	=	grid radius
T_{eV}	=	electron temperature
V_{min}	=	minimum centerline potential
V_{SCREEN}	=	screen grid potential
V_{ACC}	=	accel grid potential
V_C	=	potential at the exist of the discharge hollow cathode
η_{PROP}	=	propellant utilization efficiency
ϕ	=	plasma floating potential referenced to anode voltage

I. Introduction

Over the past 30 years, Gridded Ion Engines (GIE) have been extensively tested and proven, both within development programmes and more recently via flight operations. Within Europe, GIEs have been flown on the ESA Artemis spacecraft [1] and ESA Gravity field and steady-state Ocean Circulation Earth Explorer (GOCE) mission [2]. In 2016, ESA's Bepi-Colombo spacecraft will use GIE technology as primary propulsion for the

[1] Director, michele.coletti@mars-pace.co.uk

interplanetary cruise between Earth and Mercury [3]. The T6 Gridded Ion Engine is currently under development and qualification for the Bepi-Colombo mission and other commercial applications.

The Bepi-Colombo specification requires that the delivered thrust shall be throttleable between 75mN and 145mN. Within the Bepi-Colombo endurance test programme the thruster will be operated mainly at 145mN with periodic characterization tests at 75 and 100mN [4]. Bepi-Colombo activities have already confirmed that operation at 75mN does not impact the thruster lifetime, so the endurance testing is being performed at 145mN in order to represent worst case erosion. In addition to this the Marco Polo R (MPR) mission analysis is currently considering to reuse the Bepi-Colombo thruster as a 'back-up' system 'as-is' but with an extended thruster operating range down to 50mN.

An ESA funded activity involving QinetiQ and Mars Space Ltd is currently ongoing to evaluate the applicability of the T6 ion engine to the Marco Polo R mission performing both experimental testing and numerical modelling of the engine. A short experimental campaign has already been carried out at QinetiQ demonstrating that the T6 can deliver thrust as low as 30mN maintaining the accel grid to beam current ratio below 3%.

The ability of performing meaningful ion optics modeling of the T6 ion engine is beneficial to both the Bepi-Colombo and the MPR missions and to any other future engine applications. The goal of this paper is to validate the FFX ion optics code [5, 6] with respect to the data currently available for the T6 (beam current and accel grid current), to validate a 0D discharge model to be used to derive the discharge plasma properties at setpoint where no measurements exist and to utilize both these tools to perform lifetime simulations for thrust levels ranging from 30 to 145 mN. The work presented here is part of an on-going effort that in the near future will include comparison between the numerical simulations and the erosion measurements that will be performed as part of the Bepi Colombo endurance test campaign.

In this paper the inputs to the simulations will be presented first; after this the numerical tools will be validated and the plasma parameters extrapolated from the measured Bepi values to the MPR setpoints. Finally the grids lifetime is simulated.

II. Simulation inputs

To perform the numerical investigation of the T6 ion engine inputs are needed regarding the grid geometry and the T6 measured plasma density and temperature profile at the BepiColombo setpoints.

A. Grids geometry

The grid set consists of an accel grid and a screen grid. Both grids have an active diameter of 22 cm and are perforated with apertures placed on a hexagonal pattern.

The screen grid has an average transparency of 60% and is divided in 5 zones (Figure 1) with the inner zones being characterized by smaller aperture diameters than the outer ones. The accel grid has instead a constant aperture diameter of about 1.5 mm and a transparency of about 40%. The screen grid is manufactured in molybdenum whereas the accel grid is made of graphite.

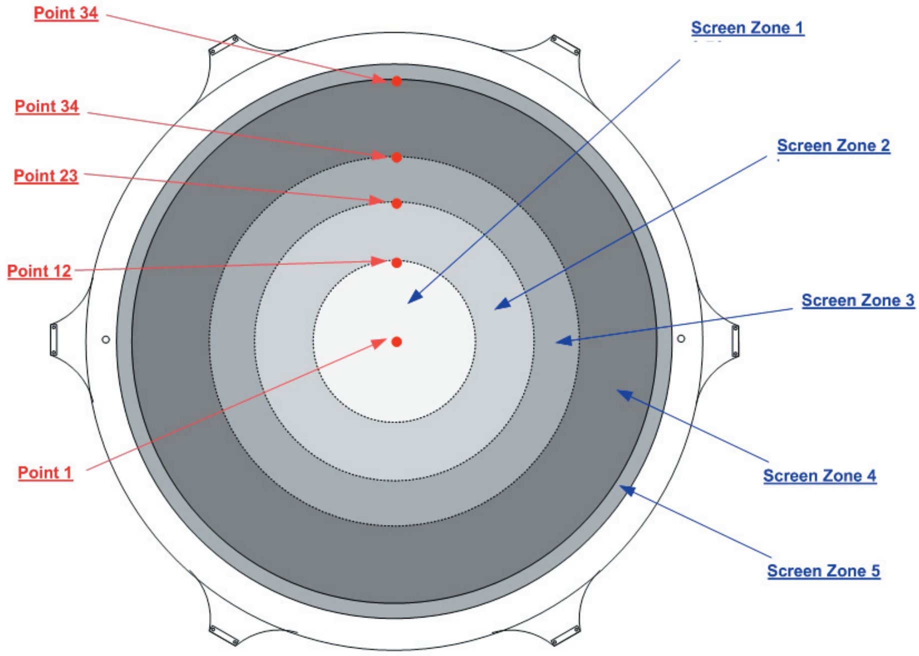

Figure 1. Screen grid zones and simulation points

To run the ion optics code the grid gap will also be needed. At present a hot grid gap measurement has never been performed. The only known grid gap is the cold gap which is reported in Figure 2 and will be used for all simulation reported in this paper.

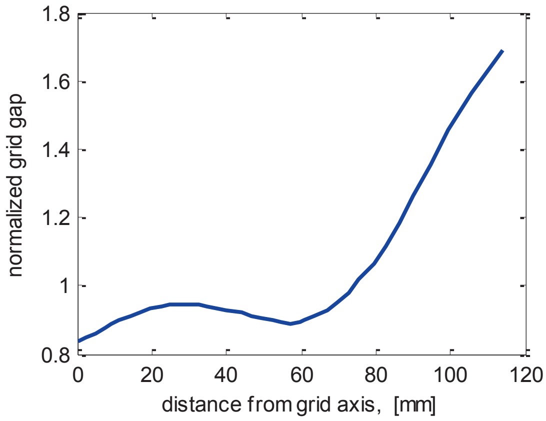

Figure 2. T6 cold grid gap

B. Plasma density and Temperature

In addition to the ion optics geometry the FFX code takes as inputs the plasma density and electron temperature, the grids potential, propellant utilization efficiency and double ion content to self consistently calculate the beamlet current and the currents to the grids.

The plasma parameters have been characterized in the frame of BepiColombo at 75, 100, 125 and 145 mN. Their trend as a function of the grid radius is reported in Figure 3. It must be noted that the uncertainty on these measurements have been quantified in ±20% and ±10% for the plasma density and electron temperature respectively.

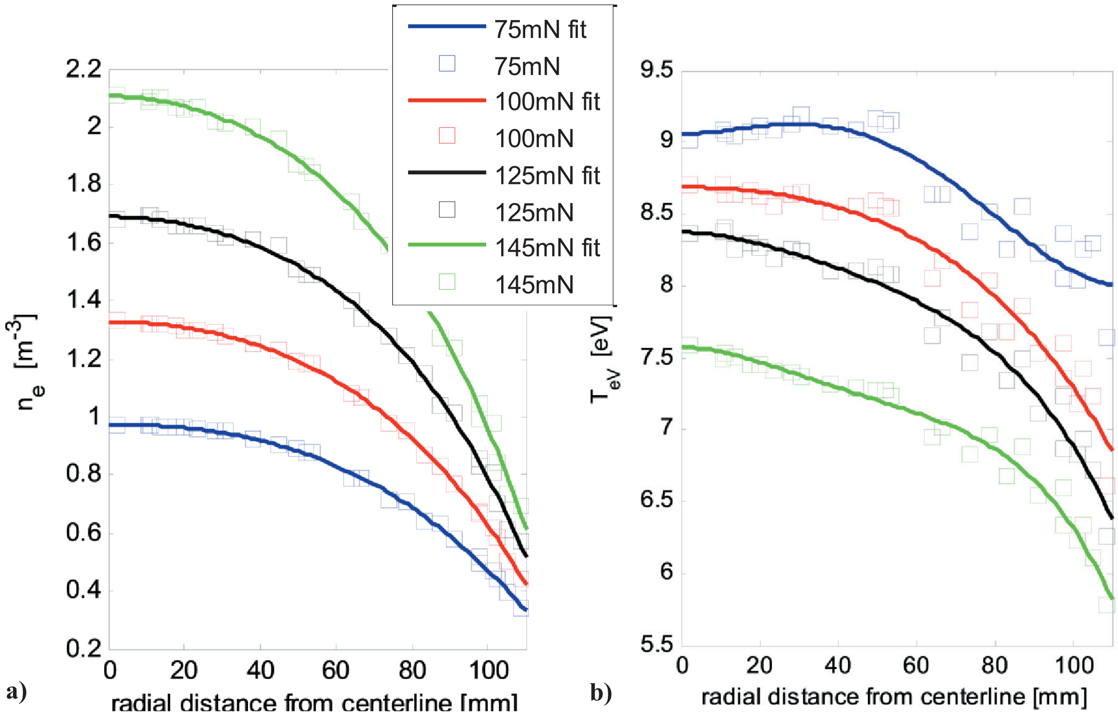

Figure 3. Measured values of the T6 plasma density and electron temperature

C. Operational set points

The T6 set points are reported in Table 1 for both the Bepi Colombo and MPR missions. It must be noted that the value of double ion content for the Bepi Colombo setpoint is the one measured at JPL and reported in [7] whereas no double ion content measurement exists yet for the MPR setpoint.

Table 1. T6 set points

Setpoint	Marco Polo R		Bepi Colombo			
	30mN	40mN	75mN	100mN	125mN	145mN
V_{SCREEN} [V]	1850	1850	1850	1850	1850	1850
V_{ACC} [V]	-265	-265	-265	-265	-265	-265
I_{BEAM} [A]	0.42	0.568	1.13	1.5	1.88	2.16
I_{Acc} [mA]	9.92	9.26	5.3	6.65	9.41	12.91
η_{PROP}	66%	74.8%	86%	88.1%	90.2%	88.9%
n++	n/a	n/a	6%	7.8%	10.25%	11%

III. Numerical tools validation

A. FFX Ion Optics Code validation

To validate the FFX code against the BepiColombo data the ion optics will be simulated using the data reported in Figure 3 and the results in terms of beam current will be compared with the experimental measurements in Table 1.

To correctly simulate the operation of the gridset several points along the grids will have to be simulated to take into account the trend of the plasma density and temperature and the fact that the screen grid aperture size changes moving from zone to zone.

Performing a trade-off between the accuracy of the results and the time needed to run all the required simulations it has been decided to simulate 5 points along the grid radius. These points are located at the grid centerline and at each zone transition as indicated in Figure 1. The simulation procedure will consist in simulating the apertures at these five points, obtaining the values of the beamlet current and accel gridlet current, dividing them by the aperture area to get the relative current densities and integrating them over the full grid to obtain the total beam current and accel grid current values. The results so obtained will then be compared with the measured values reported in Table 1. The first set of simulations has been run using the values of temperature and densities reported in Figure 3. The results obtained are reported in Figure 4 and Table 2.

Table 2 – Simulation output, nominal case

Setpoint		75 mN	100 mN	125 mN	145 mN
I_{BEAM} [A]	Simulated	0.99	1.26	1.53	1.76
	Measured	1.13	1.5	1.88	2.16
I_{ACC} [mA]	Simulated	5.81	6.89	7.45	9.57
	Measured	5.3	6.65	9.41	12.91

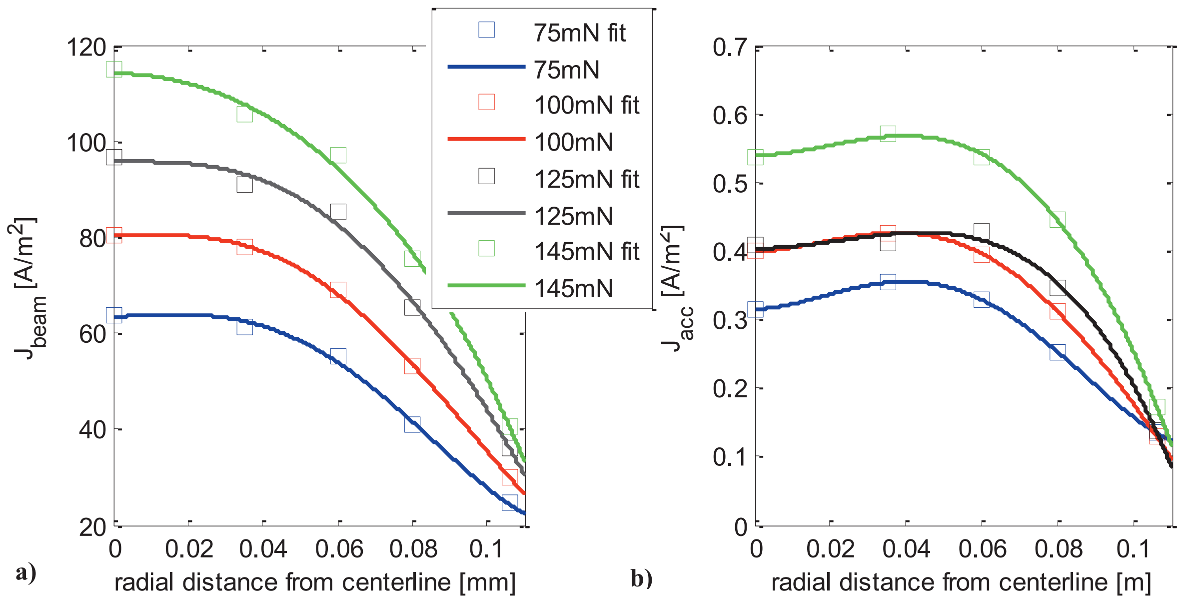

Figure 4. Beamlet current density (a) and accel gridlet current density (b) trend along the grid radius

As it can be seen smooth trends have been obtained for both the beamlet and the accel gridlet current densities. Integrating these trends over the full grid the values in Table 2 have been obtained. Comparing these with the measured values in Table 1 it can be noticed that the beam current values predicted by FFX are significantly lower than the measurements. The agreement relative to the accel grid current is also quite poor. This can be due to three causes:

- The ion optics code is not able to accurately predict I_{BEAM} and I_{ACC}
- The hot grid gap is significantly different from the cold grid gap
- The density and temperature values in Figure 3 are not correct

Considering that FFX has already been successfully used and validated with respect to measurements done on HiPEP and NEXT [5, 6] we will exclude the first possibility whereas the second and third will be investigated.

First the influence of the grid gap over the extracted current has been investigated. To increase the extracted current (moving the calculated value closer to the measured ones) the grid gap needs to be reduced. Running a sensitivity analysis it has been found that gaps smaller than 0.1 mm across the whole grid are needed to justify the observed current values. Considering that such small gap would most likely cause continuous arcing between the grids (since it corresponds to an average electric field of about 20kV/mm) we have excluded the possibility that the difference between measured and calculated values is due to the grid gap.

The only parameter left to investigate is potential errors on the plasma density and the electron temperature measurements. Considering that:

- the extracted beam current is directly proportional to the plasma density
- the extracted beam current is proportional to the square root of the electron temperature
- the error bar on the plasma density is ±20%
- the error bar on the electron temperature is ±10%

it has been decided to modify the density profiles reported in Figure 3 increasing them by a percentage correction factor until the measured values of beam current can be reproduced. The electron temperature has instead kept at its nominal value. It was found that with correction factors of about 20% to 30% a satisfactory agreement can be found between the beam current measurements and the FFX predictions as can be seen in Table 3.

It must be noted that the magnitude of the error bar provided above relative to the plasma density and electron temperature measurement is to be considered only as an indication. This is because quantifying the effects of the theoretical assumptions that have to be made to utilize Langmuir probes and post process their data in a plasma like the one of a Kaufman ion engine discharge chamber (presence of magnetic fields, high double ion content, non Maxwellian electron distribution etc) is extremely difficult. Considering this, the correction factors can be considered satisfactory and roughly in line with the expected measurement error bar.

Table 3. Simulation output, modified case

Setpoint	75 mN	100 mN	125 mN	145 mN
Density Corr Factor	16%	24%	28.5%	27%
I_{BEAM} [A]	1.129	1.51	1.89	2.14
I_{ACC} [mA]	6.73	8.69	9.83	12

Looking at Table 3 it can be seen how the accel grid currents are slightly higher than the measured values. This is due to the fact that the absolute value of the accel grid current is influenced by the propellant neutralization downstream of the engine and by the vacuum chamber background pressure.

FFX cannot self consistently take into account these effects since the beam neutralization is a very complicated problem that will require the simulation of the whole engine and neutralizer. To best fit the accel grid current it has been decided to modify the propellant utilization efficiency until a match between the measured and calculated values is obtained. The results are reported in Table 4.

Table 4. Comparison between simulated and measured I_{BEAM} and I_{ACC} values

Setpoint		75 mN	100 mN	125 mN	145 mN
Calculated by FFX	Density Corr Factor	16%	24%	28.5%	27%
	η_{PROP}	86.20%	88.18%	87.51%	84.9%
	I_{BEAM} [A]	1.129	1.51	1.89	2.14
	I_{ACC} [mA]	5.27	6.62	9.40	13
Measured	η_{PROP}	86%	88.1%	90.2%	88.9%
	I_{BEAM} [A]	1.13	1.5	1.88	2.16
	I_{ACC} [mA]	5.3	6.65	9.41	12.91

As it can be seen changes of the order of 2-3% to the propellant utilization efficiency are sufficient to closely fit the accel grid currents. It has to be noted that 3% is most likely comparable to the mass flow sensor/controller measurement error bar.

At this point a satisfactory conclusion to the validation of the FFX model has been achieved obtaining a reasonable agreement between the numerical data and the experimental measurement available.

B. 0D discharge chamber model validation

The idea behind the 0D model is to have an easy mathematical tool that can provide relatively accurate forecast on the plasma internal parameters starting from the knowledge of the engine operating parameters.

To do so the discharge chamber is modelled assuming that the values of the plasma density, electron and ion temperature and primary electron density and energy are constant within the discharge chamber volume and following what was reported by Goebel and Katz [8, 9].

The model takes as inputs the thruster and grids geometry, the operating conditions (such as beam current, anode voltage and current, propellant utilization efficiency) and thruster magnetic field topology and returns as outputs the value of the electron temperature and plasma density.

To provide the requested outputs the model will also need the values of:

- the effective area of the surfaces at cathodic potential collecting ions, A_i
- the effective area of the anode collecting primary electrons, A_p
- the plasma floating potential referenced to the anode voltage, ϕ
- the plasma potential at the discharge hollow cathode exit, V_C

From the data available from the Langmuir Probe plasma measurements performed in the frame of the Bepi Colombo program the discharge plasma is found to float at a potential that is very close to the discharge voltage. The value of ϕ is always lower than 2V and is hence negligible in comparison to the discharge voltage that is normally of the order of 30V.

The value of V_C can be assumed to be about 12V based on the measurement and modelling results available in the literature [8, 10].

Considering this we are left with only two free parameters i.e. the anode area collecting primary electrons (A_p) and the cathodic surface area collection ions (A_i). The values of these two free parameters that best fit the Bepi Colombo measurements are reported below in Table 5. The electron temperature and plasma density values reported in the table are the integral average of those reported in Figure 3 where the values of n_e have been corrected according to the factors reported in Table 4 (to be consistent with the validation of the FFX code reported in the previous section).

Table 5. Comparison between the measured plasma characteristics and the 0D model output.

Setpoint		75 mN	100 mN	125 mN	145 mN
Measured	n_e [non dim]	0.799	1.149	1.518	1.849
	T_{eV} [eV]	8.56	7.91	7.508	6.817
Calculated by the 0D model	n_e [non dim]	0.789	1.116	1.473	1.788
	error on n_e	-2.6%	-2.8%	-2.06%	-3.3%
	T_{eV} [eV]	9.06	8.41	8	7.31
	error on T_{eV}	5.8%	6.3%	6.6%	7.3%
A_p=8.986·10^{-4} m^2			A_i=0.0559 m^2		

As it can be seen the fits provide good results with errors that for the density are of the order of 2-3% and for the temperatures of 5-8%. It is instructive to compare the values of A_p and A_i to those of the anode and of the baffle and discharge chamber upstream surface.

The ratio between A_p and the anode surface is about 4% which means than only a very small fraction of the primary ions can reach the anode without having to experience an inelastic collision, resulting in an overall satisfactory magnetic confinement. This was expected since one of the features of a Kaufman discharge chamber is to have a very strong magnetic confinement that impedes (almost completely) primary electrons from reaching the anode [8].

The ratio between the total cathodic surface collecting ions (A_i) and the sum of the area of the baffle and of the upstream surface of the discharge chamber (that are the surfaces at cathode potential) area is about 1.4. Such a value should not be considered surprising since the plasma density close to the baffle is likely to be significantly higher than in the core of the discharge chamber given the proximity of the baffle to the cathode orifice.

In light of the above, we therefore have confidence that the 0D model is able to produce results that sufficiently accurately correlate to measured data in the Kaufman discharge chamber.

IV. MPR setpoints plasma parameters extrapolation

A. Average plasma density and electron temperature

Now that the 0D model has been tuned to best fit the Bepi Colombo data it will be used with the MPR low thrust setpoint data in Table 1 to derive the plasma density and electron temperature at a thrust level of 30 and 40mN. The results so obtained are reported in Table 6.

Table 6. Average plasma density and electron temperature for the MPR setpoints

Setpoint	30 mN	40 mN
n_e [non dim]	0.258	0.359
T_{eV} [eV]	9.07	9.06

B. Plasma density and electron temperature profile extrapolation

To be able to simulate the grid erosion and lifetime at 30 and 40 mN the full electron temperature and plasma density profiles will be needed. To obtain them an extrapolation law will be derived based on the Bepi Colombo data and subsequently applied to the average values derived in the previous section.

Considering that the Bepi Colombo data are relatively smooth as can be noticed in Figure 4 it has been decided to interpolate the data with a third order polynomial of the form

$$n_e = A_n r^3 + B_n r^2 + C_n r + D_n \quad (1)$$

$$T_{eV} = A_T r^3 + B_T r^2 + C_T r + D_T \quad (2)$$

Considering that the average values of T_{eV} and n_e are provided by the model a relationship has been introduced to link the value of the polynomial coefficient to the average value and in particular:

$$A_n = a_n n_{e\,mean} \quad ; \quad A_T = a_T T_{eV\,mean} \quad (3)$$

$$B_n = b_n n_{e\,mean} \quad ; \quad B_T = b_T T_{eV\,mean} \quad (4)$$

$$C_n = c_n n_{e\,mean} \quad ; \quad C_T = c_T T_{eV\,mean} \quad (5)$$

$$D_n = n_{e\,mean} - \left(\frac{2}{5} A_n r_g^3 + \frac{1}{2} B_n r_g^2 + \frac{2}{3} C_n r_g\right) \quad (6)$$

$$D_n = T_{eV\,mean} - \left(\frac{2}{5} A_T r_g^3 + \frac{1}{2} B_T r_g^2 + \frac{2}{3} C_T r_g\right) \quad (7)$$

where r_g is the grid radius. The values of the parameters in Eq. (3) – (5) have been obtained performing a least mean square fit of the Bepi Colombo data. The outcome of the fit has been positive with least mean square errors lower than 3%. The electron temperature and plasma density profiles at 30 and 40 mN can then be derived using Eq (1)-(7). The results are reported in Figure 5.

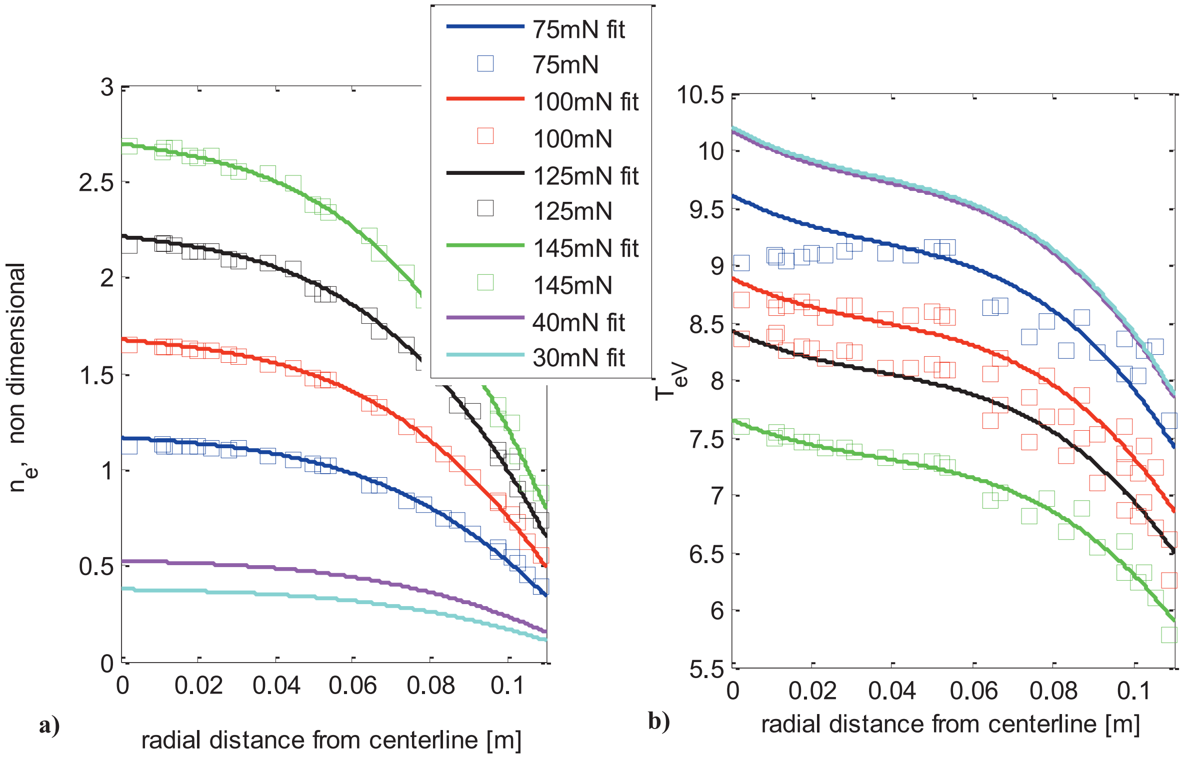

Figure 5. Computed plasma density and electron temperature profiles

C. Beam current and accel grid current simulation at the MPR setpoint

As previously done in Sec. III.A for the Bepi setpoints, FFX simulations will be run for the MPR setpoints using the n_e and T_{eV} profile in Figure 5 and compared to the data measured experimentally. The results are reported in Figure 6 together with the measured I_{ACC} and I_{BEAM} values.

Table 7. Comparison between simulated and measured I_{BEAM} and I_{ACC} values for the MPR setpoints

Setpoint		30 mN	40 mN
FFX	I_{BEAM} [A]	0.385	0.545
	I_{ACC} [mA]	5.87	5.61
Measured	I_{BEAM} [A]	0.42	0.568
	I_{ACC} [mA]	9.92	9.26

As it can be seen there is a discrepancy between the computed and measured data. Following the same process used previously in Sec III.A the plasma profile and the propellant utilization efficiency have been tuned to best fit the measurements. The results are reported in Figure 7.

Table 8. Comparison between the best fit simulated and measured I_{BEAM} and I_{ACC} values for the MPR setpoints

Setpoint		30 mN	40 mN
Calculated by FFX	Density Corr Factor	7.6%	3.7%
	η_{PROP}	61.9%	64.1%
	I_{BEAM} [A]	0.42	0.568
	I_{ACC} [mA]	9.92	9.26
Measured	η_{PROP}	66.07%	74.8%
	I_{BEAM} [A]	0.42	0.568
	I_{ACC} [mA]	9.92	9.26

As it can be seen the density correction factors found are significantly smaller than those reported in Table 5. This strengthens the validity of the 0D model and of the plasma temperature and density profile extrapolation that, using the corrected Bepi Colombo plasma density data, has predicted the plasma density and temperature profiles within an error of 7.6%. Nevertheless it has to be noted that the change in propellant utilization efficiency needed to best fit the measurements for MPR are higher than those needed for the Bepi measurement; considering the assumptions made to develop a 0D model the overall outcome can be considered satisfactory.

V. Erosion analysis

The final goal of the numerical effort reported in this paper is to simulate the lifetime of the T6 ion engine at thrust levels ranging from 30 to 145 mN covering the needs of both the Bepi Colombo and the Marco Polo R missions. To do so the T6 has been simulated using FFX at the setpoints in Table 1 using the plasma density and electron temperature trends reported in Figure 5.

It must be noted that the T6 screen grid is made of molybdenum whereas the accel grid is made of graphite. FFX at present assumes both grids to be manufactured from the same materials. Under the assumption that the main lifetime limiting factor of the ion optics is the erosion of the accel grid the simulation have been run using the sputter yield of carbon reported by Yamamura [11, 12] for both grids. Moreover it should also be noted that the double ion content for the 30 and 40mN thrust setpoint has never been measured. In the numerical simulation it will be assumed that the double ion content for this setpoint will be identical to that at 75mN.

D. Erosion sensitivity to thrust level

The erosion rates at BOL at each setpoint and for each of the points in Figure 1 are reported in Figure 6 and Figure 7. In Figure 6 the erosion rate trend along the accel grid thickness is reported whereas in Figure 7 the overall erosion rate on the upstream face, downstream face and bore of the accel grid are presented.

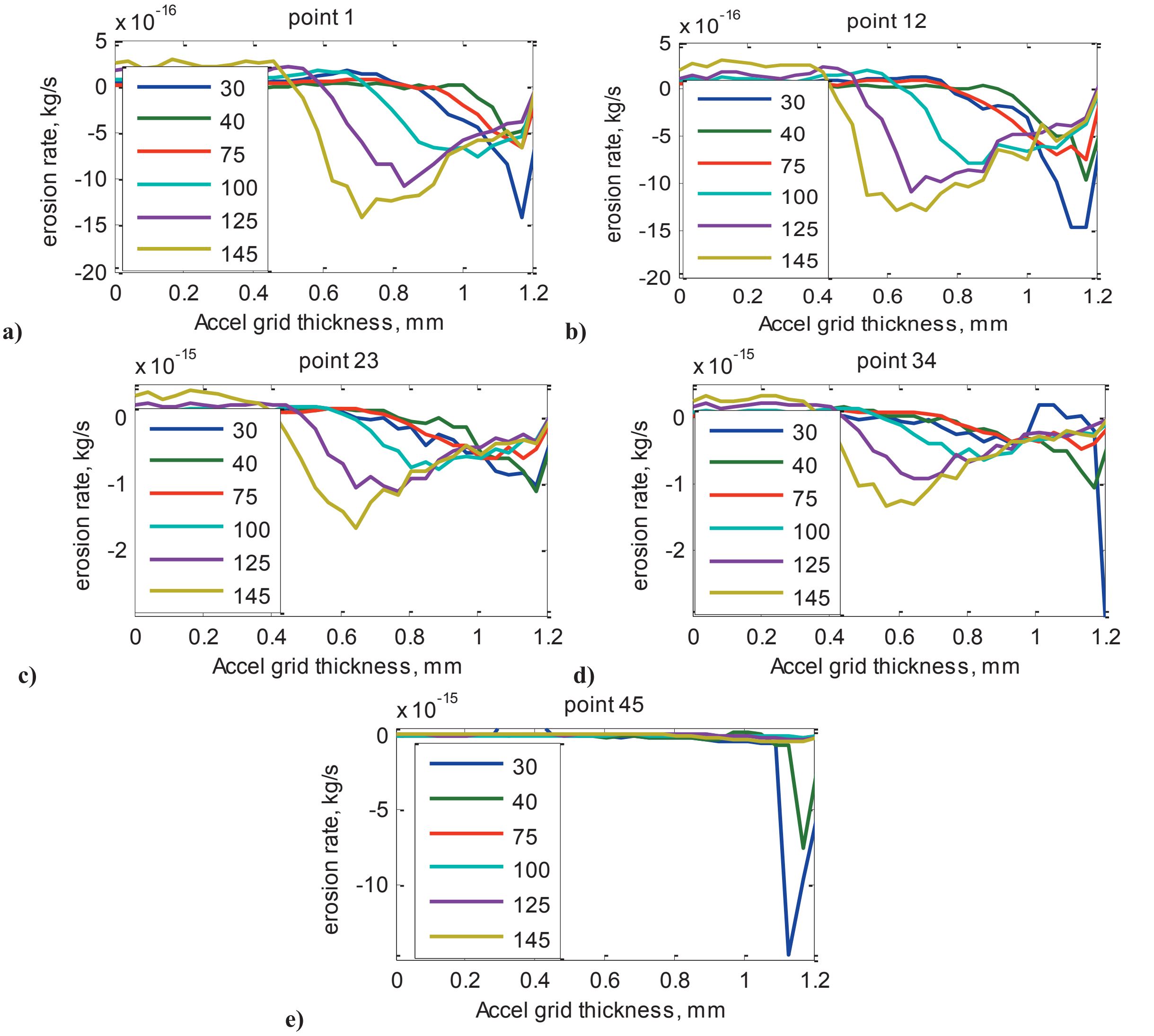

Figure 6. Erosion rate trend along an accel grid aperture for various trust levels (in mN); negative values indicate mass loss, positive values mass gain. a) zone 1, b) transition zone 1 to 2, c) transition zone 2 to 3 d) transition zone 3 to 4 e) transition zone 4 to 5

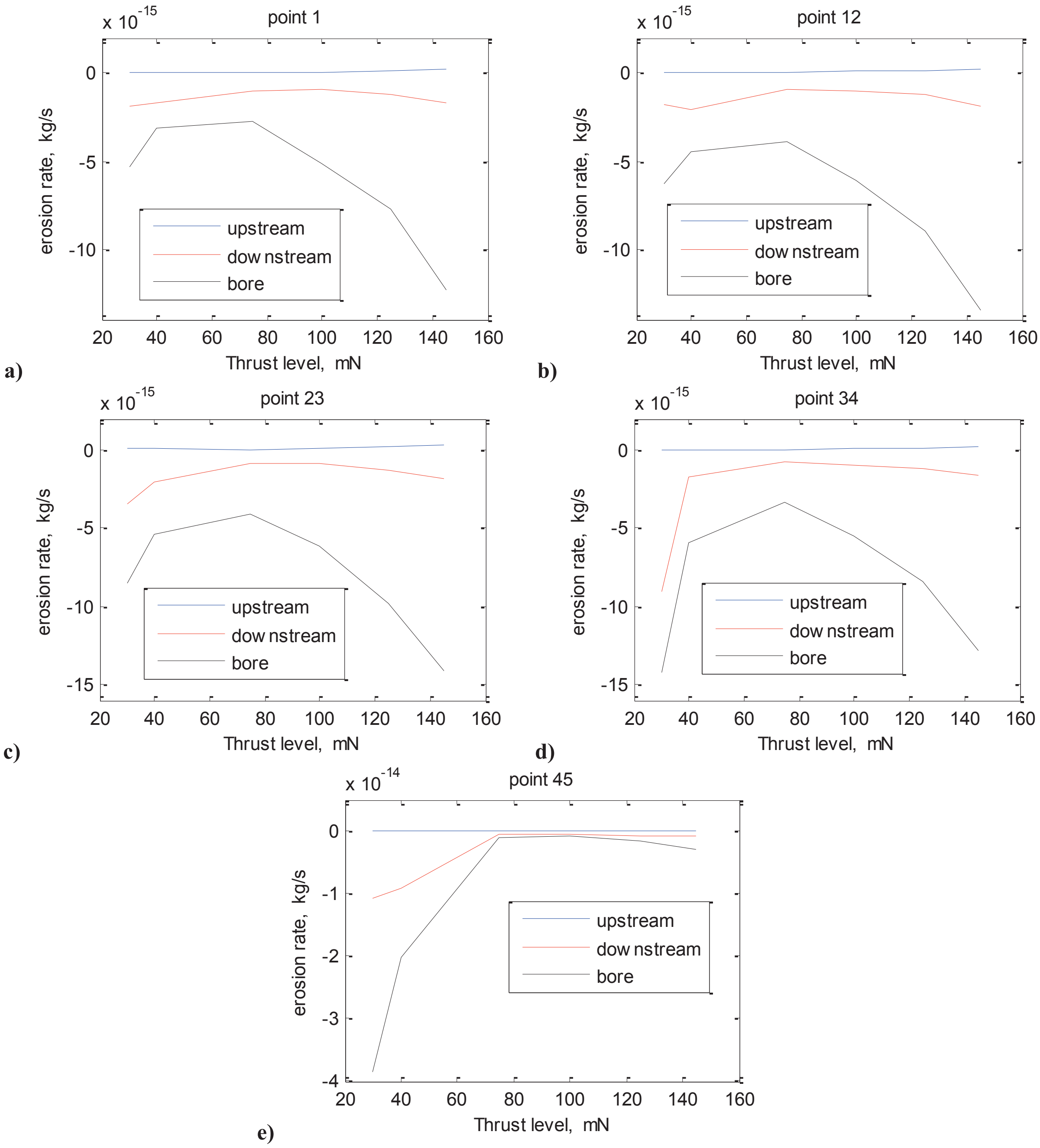

Figure 7. Erosion rates for the upstream, downstream and bore region of an accel grid aperture; negative values indicate mass loss, positive value mass gain: a) zone1, b) transition zone 1 to 2, c) transition zone 2 to 3 d) transition zone 3 to 4 e) transition zone 4 to 5

Looking at Figure 6 and Figure 7 it can be noticed that:

- The trend of the erosion rate along the accel grid axis changes significantly with the setpoint and moving from zone 1 to zone 5. In particular the trends show a maximum erosion location that tends to move downstream with decreasing thrust across the whole thrust range under investigation. This can be justified noting that a decrease in thrust corresponds to a decrease in plasma density. This gradually causes an overfocusing of the ions, changing the beamlet shape and pushing the main CEX production zone downstream. This has its maximum impact at the lowest thrust levels (30 and 40mN) and at the grid periphery (point 45) where the plasma densities are at their minimum causing a strongly over focused beamlet that generates highly localized erosion at the downstream end of the accel grid (Figure 6e).

- It should also be noted that during the T6 low thrust experimental tests operation at thrust levels lower than 30mN caused the ratio of accel to beam current to increase over 3%. Considering what has been said above this was most likely caused by direct ion impingement occurring at the grid periphery due to beamlet crossover.
- The absolute value of the erosion at this location decreases from 145 to 75 mN whereas it increases again from 75 to 30 mN. This can be justified using the same arguments presented above and moreover should not be considered surprising since the T6 was designed and optimized to deliver the performance required by the Bepi Colombo mission and not to be operated at low thrust levels.
- The erosion of the upstream face of the accel grid is normally negligible and the bore erosion is larger than the downstream erosion
- The trend of the downstream and bore erosion is almost linear in the range 75 – 145 mN whereas is clearly nonlinear if the whole 30 – 145 mN range is taken into consideration in particular showing erosion rates that increase moving from 75 to 30mN.
- The downstream and bore erosion rates change significantly by moving from the grid centerline to its periphery with the worst erosion rates happening at the transition between zone 3 and zone 4 for the high thrust regime and at the transition between zone 2 and zone 3 for the low thrust regime.

Given the very strong nonlinearity in the overall erosion rates shown in Figure 7 and considering that these erosion rates have been calculated at BOL it has been decided to run lifetime simulations for all setpoints and locations. The results are presented below in Figure 8 and Figure 9 reporting the trend of the accel grid minimum centerline potential (V_{min}) and accel grid mass respectively.

It must be noted that an end of life criterion can be based on both the value of V_{min} and/or on the accel grid mass resulting in two different end of life criteria.

- *First end of life criterion*. The ion optics end of life will be reached once the value of V_{min} increases enough to allow electrons from the ion beam to backstreaming inside the discharge chamber [13]. Such limit has been reported as EBL in Figure 9 and has been calculated according to what was reported in [8, 13] resulting in a value of about -20V.
- *Second end of life criterion*. The end of life of the ion optics will be reached when the accel grid is eroded up to the point of losing its structural integrity. We will arbitrarily assume that this will happen when 50% of the accel grid mass will be eroded.

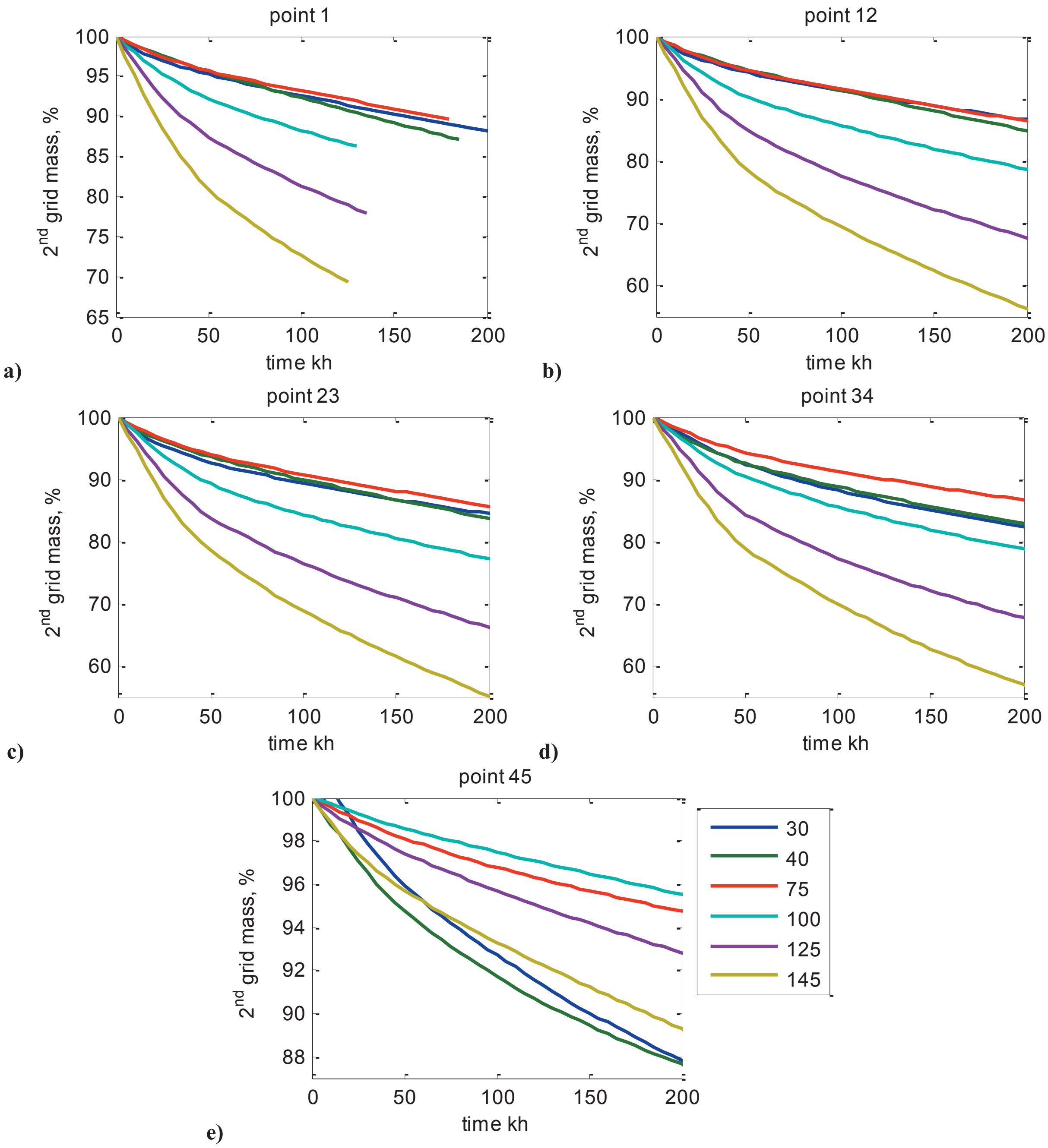

Figure 8. Accel grid mass trend during lifetime for various thrust levels (in mN): a) zone1, b) transition zone 1 to 2, c) transition zone 2 to 3 d) transition zone 3 to 4 e) transition zone 4 to 5

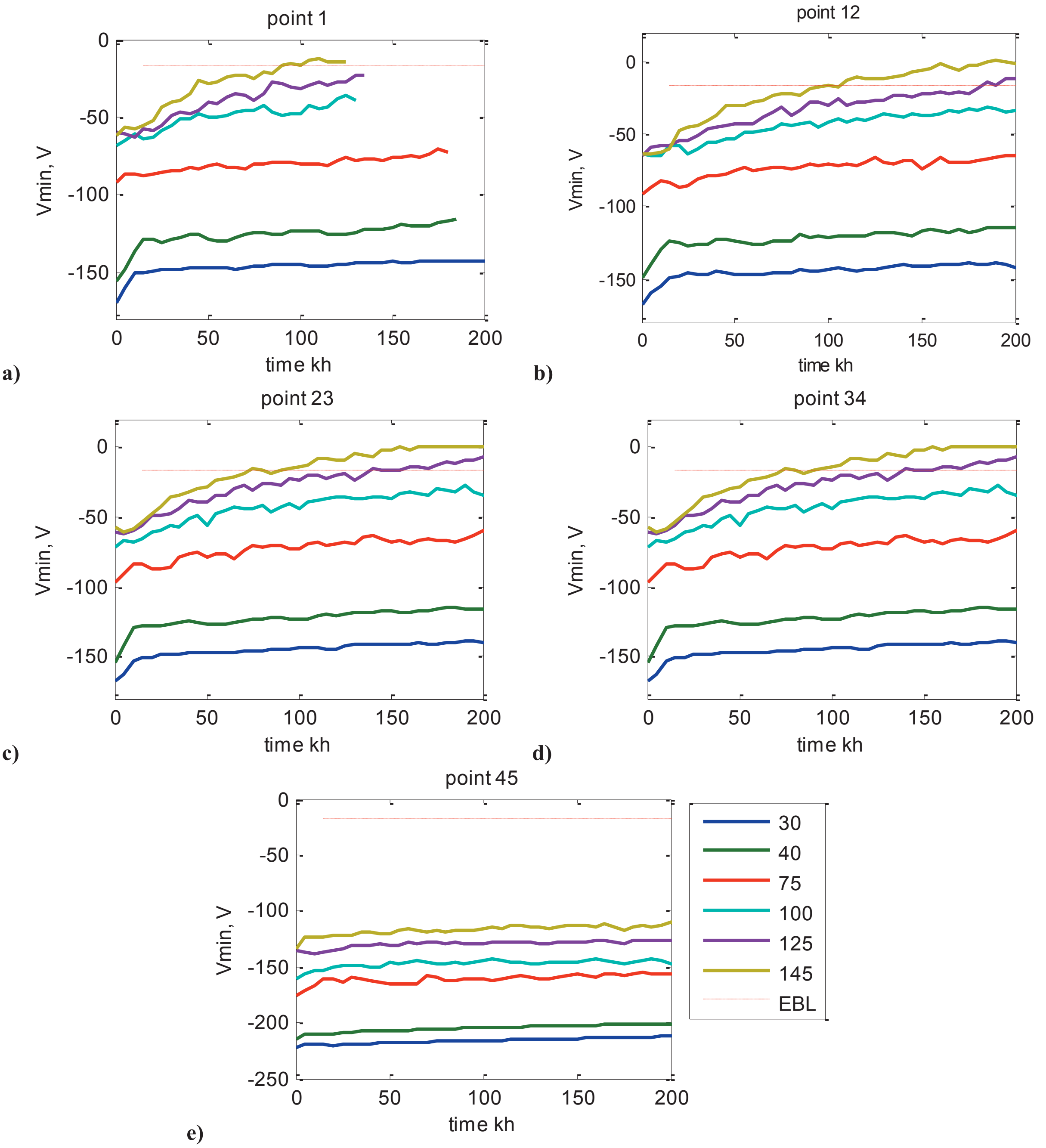

Figure 9. Minimum centerline potential trend during lifetime: a) zone1, b) transition zone 1 to 2, c) transition zone 2 to 3 d) transition zone 3 to 4 e) transition zone 4 to 5

Using the data in the figures above lifetime estimation for each zone and using both criteria reported above can be done. It must be noted that the simulations have not been run for long enough to reach the end of life in all cases given the long duration of each simulation (the simulation of one zone at one thrust setpoint takes about 1 week) hence, where needed, the data will be extrapolated until the end of life is reached according to either of the criteria above. The results are reported in Table 9 where the criterion producing the shortest life time estimate is also reported. In Table 10 the overall lifetime of the ion optics is presented for the various setpoints.

Table 9. Ion optics lifetime for various zones

	Zone 1	Zone 12	Zone 23	Zone 34	Zone 45
30 mN	1.6Mh mass	1.4Mh mass	1 Mh mass	1.5Mh mass	2.5Mh mass
40 mN	0.9Mh mass	0.9Mh mass	0.9Mh mass	1.2 Mh mass	2.7Mh mass
75 mN	0.9Mh Vmin	1Mh mass	1 Mh Vmin	0.9Mh Vmin	3.2Mh mass
100 mN	250 kh Vmin	400 kh Vmin	370 kh Vmin	700 kh Vmin	2.8 Mh mass
125 mN	150 kh Vmin	200 kh Vmin	150 kh Vmin	350 kh Vmin	1.9 Mh mass
145 mN	100 kh Vmin	100 kh Vmin	75 kh Vmin	190 kh Vmin	1.2 Mh mass

Table 10. Overall ion optics lifetime

	Lifetme	Total impulse	Criterion	Zone
30 mN	1 Mh	108 MNs	mass	23
40 mN	0.9 Mh	130 MNs	mass	12
75 mN	0.9 Mh	240 MNs	Vmin	34
100 mN	250 kh	90 MNs	Vmin	1
125 mN	150 kh	67 MNs	Vmin	1
145 mN	75 kh	39 MNs	Vmin	23

As can be seen from the figures and tables above the lifetime is longer for lower thrust levels. This is in contradiction to what was found before comparing the erosion rates at BOL in Figure 6. Nevertheless looking at the trend of the accel grid mass reported in Figure 8 it can be noticed that the erosion rates (i.e. the derivative of the mass trend) change significantly during lifetime in particular decreasing in value (the mass trends become less steep). It can also be noted that this effect is more marked for the low thrust settings especially for point 1 and 12 (close to the grid centerline).

It can also be noticed that most of the bore erosion for the 30 and 40 mN thrust level is concentrated at the downstream end of the accel grid; this is most likely due to the beamlet being over-focused with the ions crossing over the aperture centerline and generating CEX ions close to the bore downstream end. This localized erosion rate will produce a chamfer in the aperture that will either avoid further CEX ions impingement or will at least change the impingement angle consequently changing the sputter yield ultimately reducing the erosion rates.

It must also be noted that a lower thrust level means a lower extracted beamlet current hence a lower (better) value of the minimum centerline potential (due to a lower positive space charge effect [8, 13]) hence a larger margin over the occurrence of electron backstreaming. This can be clearly seen in Figure 9 where the value of V_{min} at BOL increases (is less negative) for increasing thrust level with a margin over BOL for the 30mN case that is almost 300% of that at 145mN.

In agreement with this it must be noted that the end of life is determined mainly by the change in the minimum centerline potential for thrust levels from 100 to 145 mN whereas is mainly due to a mechanical failure of the accel grid for thrusts of 40 and 30mN and depends heavily on the zone under investigation for 75mN.

Moving from the center of the grids towards the edge of the grids it has an effect on lifetime that is similar to reducing the thrust level. This is because the electron density decreases towards the grid periphery, explaining why in zone 45 the main end of life mechanism is mechanical failure of the accel grid (Table 9).

Looking now at the overall thruster lifetime it can be seen how the values derived are in general very long. While this provides confidence in the ion optics design it also means that the engine lifetime limiting mechanism might not be the ion optics erosion and in particular the accel grid erosion.

Another factor to take into account is that in these simulations the screen grid was assumed to be made of carbon and did not show any signs of erosion. In reality the screen grid is made of molybdenum and is mainly subjected to low energy sputtering from ions impacting with energies of the order of the discharge voltage (~30V) or twice that for double ions. At such energy the sputter yield of molybdenum and carbon are not yet very well defined hence more detailed analysis should be dedicated to the screen grid erosion.

Finally it must be noted that the sputter yield of carbon and most importantly its angular dependence is found to depend heavily on the type of graphite used and on its surface finish [14, 15]. Therefore to obtain very reliable simulations, sputter yield measurements should be conducted on the exact form of graphite used to manufacture the accel grid.

VI. Conclusion and Future Works

In this paper the results relative to the simulation of the T6 ion optics lifetime has been presented. Prior to carrying out such simulations the FFX code has been successfully validated with respect to the available BepiColombo measurements in terms of beam current and accel grid current. To match the values of the current to the grids the measured plasma density values had to be increased by about 20 to 30% and the propellant utilization decreased by up to 3%. Both these changes are compatible with the measurement error bars. The computed values of the beam current and accel grid current are typically within 1% of the measured values.

After this the 0D model that was used to derive the plasma density and electron temperature profile at those setpoints where no experimental data is available, has been presented. The 0D model has been successfully fitted to the Bepi Colombo data, providing results that are in very good agreement with the measurements. To obtain such agreement two free parameters have been used, the area of the anode collecting primary ions and the area of the cathodic surface collecting ions. The values found for the free parameters are in line with the theoretical expectations.

The model has then been used to derive the n_e and T_{eV} profiles at 30 and 40mN of thrust. Subsequent FFX simulations have been found that the predicted values are within 7.6% of those needed to best fit the measured beam and accel grid current values at 30 and 40mN hence increasing the confidence in the validity of the 0D model.

The T6 ion optics lifetime has been simulated at thrust levels ranging from 30 to 145mN. The calculated lifetimes have been found to be largely in excess of 50,000 hours with total impulse values ranging from 40 to 110MNs depending on the thrust level. Nevertheless these predictions should be taken with care since the sputter yield of the graphite used to manufacture the accel grid is not precisely known (the sputter yield depends on the exact type of graphite used and its surface finish) and since the screen grid erosion should also be taken into account considering the extremely long lifetimes.

Nevertheless considering that the calculated lifetimes are several times (to orders of magnitude) higher than the Bepi Colombo and Marco Polo R mission requirements (about 11.5MNs for Bepi and about 7MNs for MPR) it can be concluded with some confidence that the T6 ion optics should be well suited to meet such requirements.

Future work will include the comparison of the FFX predictions with the eroded grid profile to be measured during the Bepi Colombo lifetime test campaign[4], investigation into the most appropriate sputter yield to use for the accel grid and modelling of the screen grid erosion.

Acknowledgments

The author would like to thank QinetiQ for allowing him to use the T6 experimental data obtained during the Bepi Colombo test campaign and for the help in reviewing this paper.

References

[1] R.Killinger, R.Kukies, M.Surauer, A.Tomasetto, and L.Van Holtz. *"ARTEMIS orbit raising inflight experience with ion propulsion"*. Acta Astronautica Vol Vol 53 (Iss 4-10), 607-621. 2003.

[2] C.Edwards and N.C.Wallace. *"The T5 Ion Propulsion Assembly for Drag Compensation on GOCE"*. 2nd International GOCE user workshop, ESRIN, Frascati, Italy . 2004.

[3] N.C.Wallace. *"Testing of the Qinetiq T6 Thruster in Support of the ESA BepiColombo Mercury Mission for the ESA BepiColombo Mission"*. 4th Int Spacecraft Propulsion Conference . 2004.

[4] R.Lewis, J.Perez Luna, and F.Guarducci. *Qualification of the T6 Thruster for BepiColombo*. 34th International Electric Propulsion Conference and 6th Nano-satellite Symposium,Hyogo-Kobe, Japan . 2015.

[5] C.C.Farnell, J.D.Williams, and P.J.Wilbur. *"NEXT Ion Optics Simulation via ffx"*. NASA/CR-2003-212594 . 2003.

[6] C.C.Farnell. *"Numerical Simulation of HiPEP Ion Optics"*. 40th AIAA Joint Propulsion Conference . 2004.

[7] J.Snyder, D.M.Goebel, R.Hofer, J.Polk, N.Wallace, and H.Simpson. *"Performance Evaluation of the T6 Ion Engine"*. 46th AIAA/ASME/SAE/ASEE Joint Propulsion Conference & Exhibit, Nashville, 25-28 July . 2011.

[8] D.M.Goebel and I.Katz. *"Fundamentals of Electric Propulsion: Ion and Hall Thrusters "*. NASA JPL Space and Technology Series . 2008.

[9] D.M.Goebel, R.E.Wirz, and I.Katz. *"Analytical Ion Thruster Discharge Performance Model"*. Journal of Propulsion and Power Vol Vol. 23 (No. 5), 1055-1067. 2007.

[10] D.J.Milligan and S.B.Gabriel. *Generation of experimental plasma parameter maps around the baffle aperture of aKaufman (UK-25) ion thruster* . Vol 64, 952-968. 2009.

[11] Y.Yamamura and H.Tawara. *"Energy Dependence of Ion-Induced Sputtering Yields from Monatomic Solids at Normal Incidence"*. Atomic Data and Nuclear Data Tables Vol Vol 62 (No 2), 149-254. 1996.

[12] Y.Yamamura, Y.Itikawa, and I.Noriaki. *"Angular Dependence of Sputtering Yields of Monatomic Solids"*. Institute of Plasma Physics Vol Report N IPPJ-AM-26, 1-113. 1983.

[13] J.D.Williams, D.M.Goebel, and P.J.Wilbur. *"Analytical Model of Electron Backstreaming for Ion Thrusters"*. 39th AIAA Joint Propulsion Conference,Huntsville, Alabama . 2003.

[14] J.D.Williams, M.Johnson, and D.Williams. *"Sputter Yields of Carbon Materials under Xenon Ion Incidence"*. Plasma Processes and Polymers Vol Vol 4 (Iss 1), S633-S636. 2007.

[15] M.Tartz and H.Neumann. *"Sputter Yields of Carbon Materials under Xenon Ion Incidence"*. Plasma Processes and Polymers Vol Vol 4 (Iss 1), S633-S636. 2007.